

# Practical constitutive model for soil liquefaction

S.-S. Park & P.M. Byrne

*Department of Civil Engineering, University of British Columbia, Vancouver, B.C., Canada*

**ABSTRACT:** A practical constitutive model is presented that incorporates shear-induced effects in both loading and unloading as well as rotation effects. It is developed within a classical plasticity approach combined with a multi-laminate model. A multi-laminate model uses many mobilized planes, but the proposed model has only two mobilized planes; a maximum shear stress plane, and a horizontal plane. The application of more than one mobilized plane can intrinsically handle anisotropy as well as rotation of principal planes. The procedure focuses on simple shear conditions because they simulate field conditions under earthquake loading. The rotation effect associated with simple shear loading from a  $K_0$  consolidated state and its effect is incorporated with the Two Plane model. This constitutive model is incorporated into the dynamic coupled stress-flow finite difference program FLAC (Fast Lagrangian Analysis of Continua). It is verified by capturing the cyclic undrained behaviour of Fraser River sand. The numerical simulations under two different  $K_0$  conditions, 0.5 and 1.0 are compared with measurements.

## 1 INTRODUCTION

The characteristic liquefaction/cyclic mobility response of saturated sand is caused by shear induced plastic contraction and dilation under cyclic loading. Test data show that the response depends on stress ratio, the ratio of shear stress to normal effective stress, and whether it increases or decreases (loading or unloading). It also depends on whether the direction of the principal stresses rotates during the loading process. Plastic contraction occurs for loading below the phase transformation line ( $\phi_{pt}$ ) and dilation above. All unloading is contractive and particularly so if the previous loading has been above  $\phi_{pt}$ . If the sand is free to drain during cyclic loading, cyclic volume changes occur. If volume change is suppressed by the presence of water that cannot escape, cyclic pore pressures may result in liquefaction.

Many researchers have proposed many different types of numerical models for soil liquefaction analysis. These are mainly based on plasticity. The practicality of utilizing numerical models depends on their simplicity and robustness (Kolymbas 2000). Consequently, the practical application of models has been limited to few cases. Dafalias (1994) reviewed the constitutive models used by the predictors in the VELACS project. He divided plasticity models into 4 groups: bounding surface model, nested-surfaces model, generalized plasticity model,

and classical plasticity model. A classical plasticity based constitutive model has been developed to handle plastic unloading and principal stress rotation associated with anisotropic consolidation, or  $K_0$  state at the University of British Columbia (UBC). In terms of a mobilized plane, this model is similar to a multi-laminate model proposed by Pande & Sharma (1983) that uses many mobilized planes. The proposed model uses only two mobilized planes, a maximum shear stress plane, and a horizontal plane and links the multi-laminate model with classical plasticity. The characteristics of this model and formulation are introduced and a comparison with laboratory data is presented.

## 2 CHARACTERISTICS OF THE PROPOSED MODEL

The proposed model is an extension of a simpler model to include plastic unloading and rotation of principal planes associated with simple shear loading. UBCSAND originally considered unloading as elastic. From a practical point of view, elastic unloading may be adequate for preliminary analysis. However, laboratory data indicate that significant plastic deformation always occurs during the unloading phase. If liquefaction is expected, it is important to include plastic unloading. This is so be-

cause elastic unloading cannot capture the soil fabric collapse that occurs during stress reversal following a large stress cycle that induces dilation. In the proposed constitutive model, plastic unloading is incorporated by mobilizing plastic deformation on a horizontal plane.

A rotation of principal stresses occurs in simple shear loading and its effect depends very much on the initial  $K_0$  consolidation state. If  $K_0 = 1.0$ , then as soon as any horizontal shear stress is applied, the horizontal plane become the plane of maximum shear and essentially remains so for the rest of the loading. So that the plane of maximum shear is horizontal for the duration of loading, and there is no rotation effect. Classical plasticity with a single plane simulates this condition very well. If  $K_0 = 0.5$ , then a large shear stress acts on the 45 degree plane, and as the horizontal stress is applied, the plane of maximum shear gradually rotates and becomes approximately horizontal at failure. Thus there is a gradual rotation of principal stress during the loading process. A classical plasticity approach with a single plane cannot capture the observed response in this case. We have found that the observed response can be captured by adding a plastic contribution from the horizontal plane.

It is difficult to conduct simple shear tests at specified initial  $K_0$  values. Ishihara (1996) showed that  $K_0$  has a significant effect on liquefaction resistance of sands based on a series of torsional tests with lateral confinement. He found that  $K_0 = 1.0$  is much stiffer in terms of a cyclic stress ratio,  $\tau/\sigma_{v0}'$  where  $\sigma_{v0}'$  is the initial vertical effective stress, but similar to  $K_0 = 0.5$  in terms of a cyclic stress ratio,  $\tau/\sigma_{m0}'$  where  $\sigma_{m0}'$  is the initial mean effective stress. Iai et al. (1992) considered  $K_0$  consolidated elements using a generalized plasticity approach. They mentioned that conventional plasticity models cannot simulate  $K_0 = 0.5$  consolidated simple shear because it involves effects of rotation of principal stress axis. However, within classical plasticity, the proposed model can consider rotation effects associated with  $K_0$  simple shear loading by incorporating two mobilized planes rather than one. Numerical simulations under two  $K_0$  conditions, 0.5 and 1.0, are compared with measured liquefaction behaviour.

### 3 CONSTITUTIVE MODEL: UBCSAND2

Byrne and graduate students at UBC have developed a simple constitutive model for soil liquefaction analysis since late 1990 (Byrne et al. 1995, Puebla et al. 1997, Beaty & Byrne 1998, Byrne et al. 2004). The underlying feature of their model called UBCSAND is simplicity and robustness for practical purposes. The UBCSAND stress-strain model modifies the Mohr-Coulomb model incorporated in FLAC (Fast Lagrangian Analysis of Continua) Ver-

sion 4.0 (Itasca 2000) to capture the plastic strains that occur at all stages of loading. This model has been continuously developed to better model observed sand behaviour and include the effects of rotation of principal planes or  $K_0$  effect, and plastic unloading mentioned earlier. These two factors recently incorporated into UBCSAND are presented in this paper. It is called UBCSAND2. The formulations of this model are described in this section including plastic deformations mobilized on two planes.

#### 3.1 Elastic behaviour

Elastic behaviour is assumed isotropic and expressed in terms of bulk and shear moduli. The elastic bulk modulus,  $B^e$ , and shear modulus,  $G^e$ , are stress level dependent and described by the following relations, where  $k_B$  and  $k_G$  are modulus numbers,  $P_A$  is atmospheric pressure, and  $\sigma'_m$  is the mean effective stress:

$$B^e = k_B \cdot P_A \cdot \left( \frac{\sigma'_m}{P_A} \right)^{0.5} \quad (1)$$

$$G^e = k_G \cdot P_A \cdot \left( \frac{\sigma'_m}{P_A} \right)^{0.5} \quad (2)$$

#### 3.2 Plastic behaviour mobilized on maximum shear stress plane

The formulation is based on classical plasticity. Yield loci are assumed to be radial line of constant stress ratio as shown in Figure 1 and expressed by

$$f_1 = \tau_1 - \sigma'_m \cdot \sin \phi_{m1} \quad (3)$$

where  $\tau_1$  = the maximum shear stress, and  $\phi_{m1}$  = the friction angle mobilized on the maximum shear stress plane. Reloading induces plastic response but with a stiffened plastic shear modulus. The plastic shear modulus relates the shear stress and the plastic shear strain and is assumed to be hyperbolic with stress ratio as shown in Figure 2. Moving the yield locus from A to B in Figure 1 induces a plastic shear strain increment,  $d\gamma^P$ , as shown in Figure 2, and is controlled by the plastic shear modulus,  $G^P$ . The associated plastic volumetric strain increment,  $d\varepsilon_v^P$ , is obtained from the dilation angle  $\psi_1$ :

$$d\varepsilon_v^P = d\gamma^P \cdot \sin \psi_1 \quad (4)$$

The dilation angle is based on laboratory data and energy considerations and is approximated by

$$\sin \psi_1 = \sin \phi_{m1} - \sin \phi_{cv} \quad (5)$$

where  $\phi_{cv}$  is the phase transformation or constant volume friction angle and  $\phi_{m1}$  describes the current

yield locus. A negative value of  $\psi_1$  corresponds to contraction. Contraction occurs for stress states below  $\phi_{cv}$  and dilation above. Additional information on earlier version of UBCSAND is presented by Byrne et al. (2004).

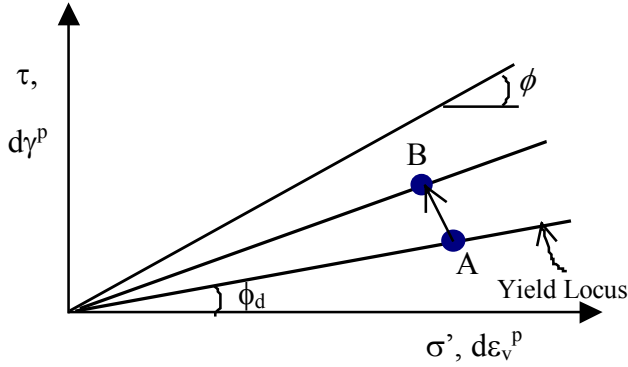


Figure 1. Yield locus of UBCSAND model.

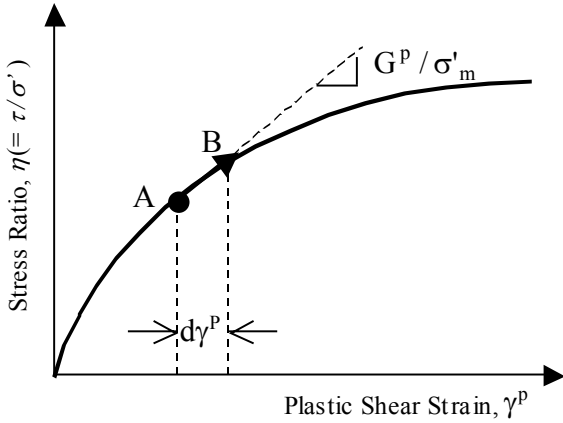


Figure 2. Hyperbolic hardener of UBCSAND model.

### 3.3 Plastic behaviour mobilized on horizontal plane

Yield loci mobilized on a horizontal plane have the same shape as for the maximum shear stress plane and expressed by

$$f_0 = \tau_0 - \sigma'_m \cdot \sin \phi_{m0} \quad (6)$$

where  $\tau_0$  = the shear stress acting on a horizontal plane, and  $\phi_{m0}$  = the friction angle mobilized on a horizontal plane. A horizontal plane will contribute not only a loading component but also plastic unloading. The plastic volumetric strain increment and a dilation angle are similar to those in Equations 4 and 5. However, the dilation angle,  $\sin \psi_0$ , is based on a mobilized angle on a horizontal plane,  $\sin \phi_{m0}$  and expressed by

$$\sin \psi_0 = \sin \phi_{m0} - \sin \phi_{cv} \quad (7)$$

### 3.4 Hardening rule

The hardening rules are similar for both maximum shear stress and horizontal planes. The only difference is the stress ratio,  $\eta$ . The plastic properties used by the model are the peak friction angle  $\phi_p$ , the constant volume friction angle  $\phi_{cv}$ , and plastic shear modulus  $G^p$ , where

$$G^p = G_i^p \cdot \left(1 - \frac{\eta}{\eta_f} R_f\right)^2 \quad (8)$$

$G_i^p = \alpha G^e$  and  $\alpha$  depends on relative density,  $\eta$  ( $= \tau_1/\sigma'_m$  or  $\tau_0/\sigma'_m$ ) is the stress ratio,  $\eta_f$  is the stress ratio at failure, and  $R_f$  is the failure ratio used to truncate the hyperbolic relationship.

For loading on the plane of maximum shear, the position of the yield locus  $\phi_d$  is initially specified for each element. As the stress ratio increases and plastic strain is predicted, the yield locus for that element is pushed up by an amount  $d\phi_d$  as given by Equation 9.

$$d\phi_d = \left(\frac{G^p}{\sigma'_m}\right) \cdot d\gamma^p \quad (9)$$

Upon unloading, plastic deformation is controlled by conditions on the horizontal plane using an incremental formulation of Equation 6 and expressed in Equation 10. The initial yield locus is set at the stress reversal point C in Figure 3 and unloading predicted based on Equation 10 until the shear stress changes sign, or reversal occurs. During unloading and reloading, plastic shear modulus based on modified shear stresses (i.e.  $\tau^* = \tau_r - \tau$  for unloading and  $\tau^* = \tau_r + \tau$  for reloading) and shear stress at failure (i.e.  $\tau_f^* = \tau_r + \tau_f$ ) is given by Equation 11 and illustrated in Figure 3. Reloading then occurs with a stiffened modulus:

$$df_0 = d\tau_0 - d\sigma'_m \cdot \sin \phi_{m0} - G^p \cdot d\gamma^p = 0 \quad (10)$$

$$G^p = G_i^p \cdot \left(1 - \frac{\eta^*}{\eta_f^*} R_f\right)^2 \quad (11)$$

where  $\eta^*$  and  $\eta_f^*$  are modified stress ratios based on modified shear stress  $\tau^*$  and  $\tau_f^*$  as shown in Figure 3.

The shear volume coupling can be determined by Equation 12 through dilation angle  $\sin \psi$ . Based on this relationship the plastic volume change during all stages is determined as illustrated in Figure 4. During unloading the amount of volume change is not influenced by the stress ratio level (i.e.  $\sin \psi = \sin \phi_{cv}$ ).

$$\frac{d\epsilon_v^p}{|d\gamma^p|} = \sin \psi = (\eta - \sin \phi_{cv}) \quad (12)$$

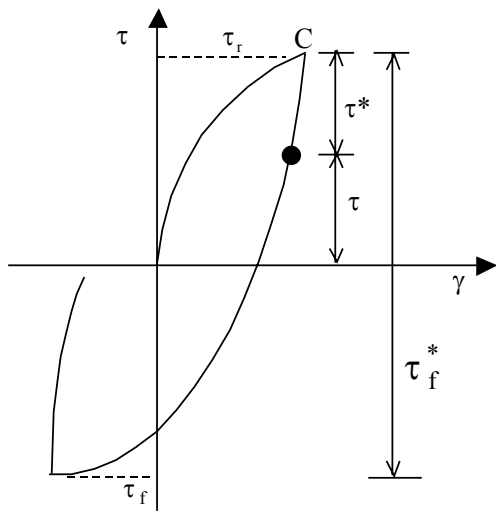


Figure 3. Stress ratio during unloading and reloading.

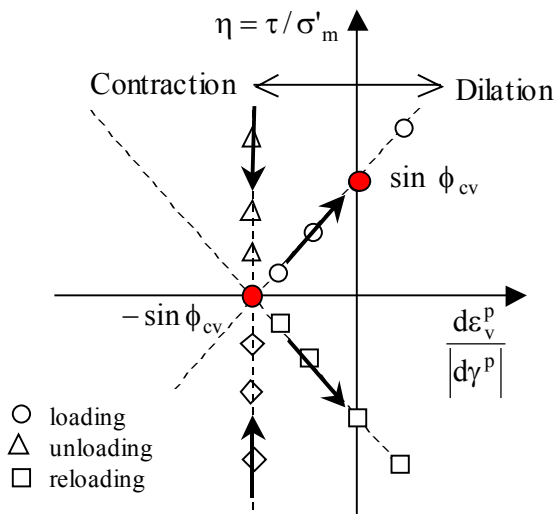


Figure 4. Shear volume coupling.

To account for principal stress rotation during loading and reloading, plastic strains on the horizontal plane are also considered during loading as described above for unloading.

The response of sand is controlled by the skeleton behaviour. A fluid (air water mix) in the pores of the sand acts as a volumetric constraint on the skeleton if drainage is curtailed. It is this constraint that causes the pore pressure rise that can lead to liquefaction. Provided the skeleton or drained behaviour is appropriately modeled under monotonic and cyclic loading conditions, and the stiffness of the pore fluid ( $B_f$ ) and drainage are accounted for, the liquefaction response can be predicted. This concept is incorporated in UBCSAND2.

#### 4 UBCSAND2 CALIBRATION

The elastic and plastic parameters are highly dependent on relative density, which must be consid-

ered in any model calibration. These parameters can be selected by calibration with laboratory test data. The response of the model can also be compared to a considerable database for triggering of liquefaction under earthquake loading in the field. This database exists in terms of penetration resistance, typically from cone penetration (CPT) or standard penetration (SPT) tests. A common relationship between  $(N_1)_{60}$  values from the SPT and the cyclic stress ratio that triggers liquefaction for a magnitude 7.5 earthquake is given by Youd et al. (2001). Comparing laboratory data based on relative density to field data based on penetration resistance relies upon an approximate conversion, such as that proposed by Skempton (1986):

$$35 < \frac{(N_1)_{60}}{D_r^2} < 60 \quad (13)$$

Model parameters based on penetration resistance and field observation may be useful for field conditions where it is very difficult to retrieve and test a representative sample. However, this indirect method is not appropriate for simulation of centrifuge models. Calibrations for this case should be based on direct laboratory testing of samples that are prepared in the same manner as the centrifuge model.

##### 4.1 Calibration with constant volume simple shear tests

A series of simple shear tests was performed on Fraser River sand at UBC and used as a database to calibrate the numerical model element response. Test data are available on web site (<http://www.civil.ubc.ca/liquefaction/>). The samples were prepared by air pluviation method, which is normally adopted in centrifuge tests. The details including test results can be found in Sriskandakumar's MASc thesis (2004). All samples were placed at  $D_r = 34\%$  and densified to 40% and 44% under applied pressures of 100 kPa and 200 kPa, respectively. Samples were then subjected to cyclic shear for a range of cyclic stress ratios under constant volume conditions that simulate undrained response. Tests were carried out for four different CSRs (Cyclic Stress Ratio), 0.08, 0.1, 0.12 and 0.15. Typical results of measured response of  $D_{rc} = 40\%$  for  $CSR = 0.1$  are shown in Figures 5a and 5b. Test data are shown as the heavy lines. The light lines are the numerical predictions for  $K_0 = 0.5$ . When  $CSR = 0.1$ , liquefaction occurred in 6 cycles. It is observed that the first and last cycles generated large excess pore pressures. Once the pore pressure ratio reached unity large cyclic strains developed referred to as cyclic mobility.

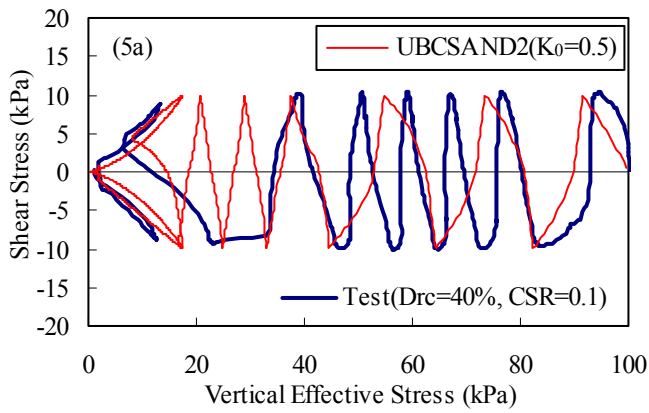


Figure 5a. Predicted stress path under  $K_0 = 0.5$  and test result.

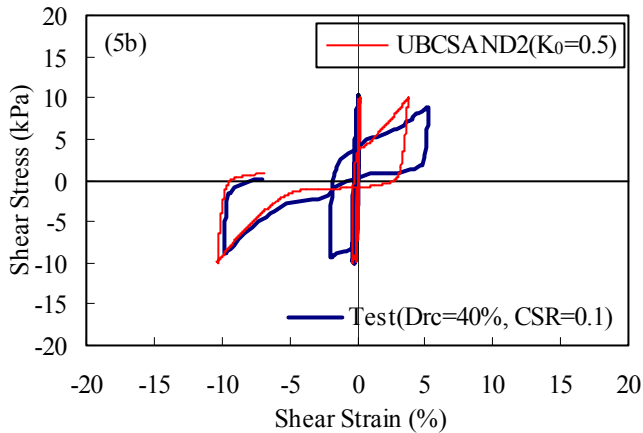


Figure 5b. Predicted stress-strain curve under  $K_0 = 0.5$  and test result.

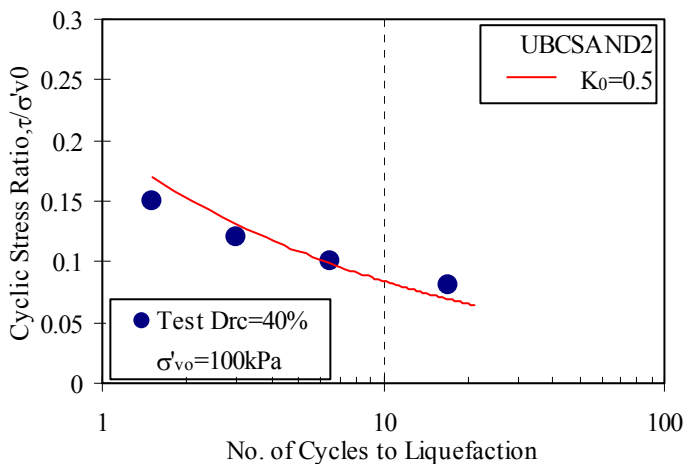


Figure 6. Predicted liquefaction resistance under  $K_0 = 0.5$  and test result in terms of  $\tau/\sigma'_{v0}$ .

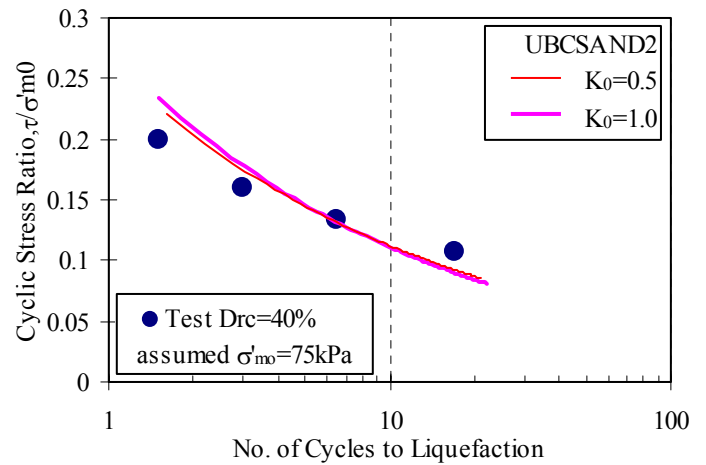


Figure 7. Predicted liquefaction resistance in terms of  $\tau/\sigma'_{m0}$  under  $K_0 = 0.5$  and  $1.0$  and test result.

The CSR versus number of cycles to liquefaction is shown in Figure 6. Liquefaction was defined as  $\gamma > 3.75\%$ , and at this point  $R_u$  (pore pressure ratio) is 90 - 95 %.

The calibration was carried out in the same way as the tests, i.e. under constant volume. The test sample was subjected to an initial vertical stress of 100 kPa under  $K_0$  conditions. It was assumed that the initial horizontal stress in the test was 50 kPa, i.e.,  $K_0 = 0.5$ . The same initial stresses were assumed in the numerical simulation. A single element was used. The elastic and plastic parameters selected for calibration were the same for all cases having the same  $D_r$ . The predicted stress-strain and stress paths for  $K_0 = 0.5$  and  $CSR = 0.1$  are shown in Figures 5a and 5b as “light” lines. The predictions generally give a reasonable representation of the observed response including plastic unloading, sudden drop of effective stress during stress reversal after dilation, and cyclic mobility.

If test condition were  $K_0 = 0.5$ , the predicted triggering of liquefaction shows a good agreement with measurements as shown in Figure 6. The predicted triggering of liquefaction for both  $K_0 = 0.5$  and  $1.0$  are shown in Figure 7. To make this comparison, the stress ratio was expressed in terms of  $\tau/\sigma'_{m0}$ . Predicted response for both  $K_0 = 0.5$  and  $1.0$  gave similar liquefaction resistance to measurements as illustrated in Figure 7. This is consistent with Ishihara’s findings (1996). Test data were assumed to have  $\sigma'_{m0} = 75$  kPa.

## 5 SUMMARY

A refined UBCSAND model called UBCSAND2 was presented. The proposed model addressed two additional features; rotation of principal planes and plastic unloading. It uses two mobilized planes; a maximum shear stress plane, and a horizontal plane.

The model was calibrated based on constant volume simple shear tests and showed the same characteristic response as observed in the physical tests. The model captured the soil fabric collapse during stress reversal after dilation and general cyclic soil behaviour including cyclic mobility after triggering of liquefaction. The model can be used in the design of liquefaction remediation measures involving densification and drainage.

## ACKNOWLEDGEMENT

Authors acknowledge that a series of simple shear tests for numerical model validation have been carried out by Mr. Sriskandakumar under the supervision of Dr. Wijewickreme at UBC.

## REFERENCES

- Beaty, M. & Byrne, P.M. 1998. An effective stress model for predicting liquefaction behaviour of sand. *Geotechnical Earthquake Engineering and Soil Dynamics III*. Edited by P. Dakoulas, M. Yegian, and R Holtz (eds.), ASCE, Geotechnical Special Publication 75 (1): 766-777.
- Byrne, P.M., Park, S.-S., Beaty, M., Sharp, M., Gonzalez, L. & Abdoun, T. 2004. Numerical modeling of liquefaction and comparison with centrifuge tests. *Can. Geotech. Journal*, Vol. 41, No. 2: 193-211.
- Byrne, P.M., Roy, D., Campanella, R.G. & Hughes, J. 1995. Predicting liquefaction response of granular soils from pressuremeter tests. ASCE National Convention, San Diego, Oct. 23-27, ASCE, Geotechnical Special Publication 56: 122-135.
- Dafalias, Y.F. 1994. Overview of constitutive models using in VELACS. *In Proceedings of the International Conference on the Verification of Numerical Procedures for the Analysis of Soil Liquefaction Problems*, Balkema, Rotterdam, the Netherlands, Vol. 2: 1293-1303.
- Iai, S., Matsunaga, Y. and Kameoka, T. 1992. Analysis of undrained cyclic behavior of sand under anisotropic consolidation. *Soils and Foundations*, Vol. 32, No. 2: 16-20.
- Ishihara, K. 1996. *Soil behaviour in earthquake Geotechnics*, Clarendon Press, Oxford.
- Itasca 2000. FLAC, version 4.0. Itasca Consulting Group Inc., Minneapolis.
- Kolymbas, D. 2000. The misery of constitutive modelling. *Constitutive modelling of granular materials*. Edited by Dimitrios Kolymbas: 11-24.
- Pande, G.N. & Sharma, K.G. 1983. Multi-laminate model of clays-a numerical evaluation of the influence of rotation of the principal stress axes. *Int. Journal for Numerical and Analytical Methods in Geomechanics*, Vol. 7: 397-418.
- Puebla, H., Byrne, P.M. & Phillips, R. 1997. Analysis of CANLEX liquefaction embankments: prototype and centrifuge models. *Can. Geotech. Journal*, Vol. 34, No. 5: 641-657.
- Skempton, A.W. 1986. Standard penetration test procedures and the effects in sands of overburden pressure, relative density, particle size, ageing and overconsolidation, *Geotechnique* 36, No. 3: 425-447.
- Sriskandakumar, S. 2004. Cyclic loading response of Fraser River sand for validation of numerical models simulating centrifuge tests. MASC Thesis, Department of Civil Engineering, UBC.
- Youd, T.L., Idriss, I.M., Andrus, R.D., Arango, I., Castro, G., Christian, J.T., Dobry, R., Finn, W.D.L., Harder Jr., L.F., Hynes, M.E., Ishihara, K., Koester, J.P., Liao, S., Marcuson III, W.F., Martin, G.R., Mitchell, J.K., Moriwaki, Y., Power, M.S., Robertson, P.K., Seed, R.B. & Stokoe, K.H. 2001. Liquefaction Resistance of Soils: Summary Report from the 1996 NCEER and 1998 NCEER/NSF Workshops on Evaluation of Liquefaction Resistance of Soils. *Journal of Geotechnical and Geoenvironmental Engineering*, 127(10): 817-833.